# Enhanced Physical Interaction Performance for Compliant Joint Manipulators using Proxy-based Sliding Mode Control

Navvab Kashiri[1], Nikos G. Tsagarakis[1],
Michäel Van Damme[2], Bram Vanderborght[2] and Darwin G. Caldwell[1]
[1]*Department of Advanced Robotics, Istituto Italiano di Tecnologia, Genova, Italy*
[2]*Department of Mechanical Engineering, Vrije Universiteit Brussel, Brussels, Belgium*

Keywords: Proxy-based Sliding Mode Control, Physical Human-robot Interaction, Flexible Joint Manipulators, Torque Control, Compliant Joints, Linear-quadratic Optimal Control, Position Control, Underactuated Systems.

Abstract: The use of typical position controllers for robots working around humans can involve some risks when unintended physical human-robot interactions occur. In order to benefit from a proper tracking performance during normal operations, and a smooth and damped recovery from position errors due to contacts with external objects/agents, Proxy-based Sliding Mode Control was proposed. While the efficacy of this controller in fully actuated manipulators was discussed, the employment of this controller in underactuated systems has not been studied so far. This paper introduces a control scheme to implement this controller in a class of underactuated systems. Specifically, the control of flexible joint manipulators possessing passive elastic elements in series with motors is studied. The formulation of Proxy-based Sliding Mode Control is adopted according to the stability requirements of this type of dynamic systems, and a torque controller required for the regulation of the the output torque of actuation units is designed using the Feedback Linearization and the Linear Quadratic optimal control approach. The performance of the proposed scheme is demonstrated in dynamic simulation of an anthropomorphic compliant arm.

## 1 INTRODUCTION

The employment of robots for different purposes and in various environments has attracted the growing attention of researchers during the last decade. The extension of robotic applications beyond industrial environment requires robots with intrinsic characteristics respecting the prerequisites of tasks. However, traditional robots are typically driven by actuators comprised of position/velocity control systems with large gains and high reduction transmission units which are quite stiff and non-back-drivable. The output mechanical impedance of robots driven by such actuation units will be very high due to large reflected inertia of drives and the rigidity of transmission elements. The performance of these robots is therefore limited in terms of mechanical robustness, and flexibility in respecting the requirements of different tasks such as interactions with external agents and objects. Hence, the development of new actuation units for robotic systems has been widely explored.

The incorporation of passive elastic elements into the transmission system of traditional actuators was proposed to suppress difficulties brought by stiff actuation systems (Tsagarakis et al., 2009). Adding flexibility to drive units reduces the output impedance, amplifies the robustness, and enhances the performance of the robot when it operates in unstructured environments and when it interacts with humans (Bicchi et al., 2001). The passive elasticity can amplify the peak output torque (Paluska and Herr, 2006; Mathijssen et al., 2013) which can be also exploited for explosive motions (Chen et al., 2013a; Braun et al., 2013).

The incorporation of passive elastic elements into the actuation units, however, increases the complexity of the system, thereby sophisticating the control scheme required for achieving a suitable tracking performance. Hence, the control of flexible joint robots has been widely studied (Ozgoli and Taghirad, 2006; Chen et al., 2013b), although a majority of these methods are highly model-based and/or requires high order derivatives resulting in implementation

Kashiri N., Tsagarakis N., Van Damme M., Vanderborght B. and Caldwell D..
Enhanced Physical Interaction Performance for Compliant Joint Manipulators using Proxy-based Sliding Mode Control.
DOI: 10.5220/0005063201750183
In *Proceedings of the 11th International Conference on Informatics in Control, Automation and Robotics* (ICINCO-2014), pages 175-183
ISBN: 978-989-758-040-6

difficulties. These issues motivated roboticists to develop variable impedance actuators (Vanderborght et al., 2013) which can be typically considered in two categories: variable stiffness actuators (Catalano et al., 2011; Tsagarakis et al., 2011; Vanderborght et al., 2011), and variable damping actuators (Garcia et al., 2011; Laffranchi et al., 2011; Radulescu et al., 2012).

A stable Proportional-Derivative (PD) based controller plus off-line gravity compensation for flexible joint manipulators was developed in (Tomei, 1991). The controller is relied upon the control of desired motor position derived from the static motion equations of links. An improvement to this approach was proposed in (De Luca et al., 2005) by means of the on-line compensation of gravity through a 'gravity-biased' modification of the motor position feedback. A novel approach for the control of such dynamic systems was proposed in (Albu-Schäffer et al., 2012) that comes from the idea of controlling an equivalent link position that approaches to the actual state, and also compensating the gravitational torque using the equivalent state.

In the way towards a safer and friendly human-robot interaction (Bicchi et al., 2001), Proxy-based Sliding Model Control (PSMC) approach was introduced in (Kikuuwe and Fujimoto, 2006), which was employed for a pneumatic actuated arm in (Van Damme et al., 2009; Beyl et al., 2009) and an electro-pneumatic powered platform in (Prieto et al., 2013). In (Kikuuwe et al., 2010), this control approach was elaborated as a safer extension to the conventional Proportional-Integral-Derivative (PID) controller, and the corresponding stability proof was shown. The performance of this efficacious approach was presented for fully actuated manipulators; however the employment of this method for passively actuated manipulators has not been discussed so far.

This paper studies the PSMC approach for flexible joint manipulators. The control scheme is developed in joint space as it was shown that this controller achieves a quite higher tracking performance when implemented in joint space rather than that in task space (Van Damme et al., 2009). The dynamic equations of this class of underactuated systems is first introduced. A position control approach for this class of dynamic systems (Albu-Schäffer et al., 2012) is presented, and the PSMC approach formulation is adopted according to stability considerations in passively actuated manipulators. A novel torque controller required for the implementation of the PSMC scheme is also designed based on the Feedback Linearization approach and the use of the Linear Quadratic (LQ) optimal method. The performance of proposed scheme is evaluated in dynamic simulations of a flexible joint arm.

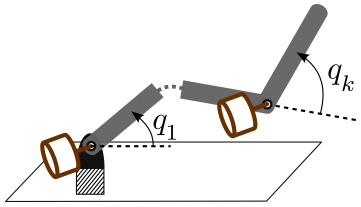

Figure 1: Schematic of a $k-$link serial manipulator.

The rest of this paper is structured as follows: the dynamic modeling of aforesaid manipulators is presented in Section 2. The control scheme including position control, PSMC and torque control are discussed in Section 3. The description of simulated manipulator and simulation results presenting the validity of proposed scheme are introduced in Section 4. Finally, section VI addresses the conclusion and future works.

## 2 DYNAMIC MODELING

Given a $k-$link serial manipulator, shown in Fig. 1, the dynamic equations of this nonlinear system can be described using Euler-Lagrange method as (Ortega, 1998)

$$\frac{d}{dt}\left(\frac{\partial \mathcal{L}(\boldsymbol{x},\dot{\boldsymbol{x}})}{\partial \dot{\boldsymbol{x}}}\right) - \frac{\partial \mathcal{L}(\boldsymbol{x},\dot{\boldsymbol{x}})}{\partial \boldsymbol{x}} + \frac{\partial \mathcal{F}(\dot{\boldsymbol{x}})}{\partial \boldsymbol{x}} = \boldsymbol{u}, \quad (1)$$

where $\boldsymbol{x} \in \Re^n$ shows the vector of generalized coordinates $(n \geq k)$, $\boldsymbol{u} \in \Re^n$ is the vector of generalized control input torques, $\mathcal{F}$ is the Rayleigh dissipation function, and $\mathcal{L}(\boldsymbol{x},\dot{\boldsymbol{x}})$ symbolizes the Lagrangian function which is defined by

$$\mathcal{L}(\boldsymbol{x},\dot{\boldsymbol{x}}) = \mathcal{T}(\boldsymbol{x},\dot{\boldsymbol{x}}) - \mathcal{U}(\boldsymbol{x}), \quad (2)$$

where $\mathcal{T}(\boldsymbol{x},\dot{\boldsymbol{x}})$ shows the kinetic energy function and $\mathcal{U}(\boldsymbol{x})$ is the potential energy function.

Manipulator fully powered by compliant actuators possess as many passive degrees of freedom (DOFs) (link positions $\boldsymbol{q} = [q_1,..,q_k]$) as active ones (motor positions $\boldsymbol{\theta} = [\theta_1,..,\theta_k]$), i.e. $n = 2k$. Fig. 2 demonstrates the mechanical model of an actuation unit of such systems. Having defined the vector of generalized coordinates as $\boldsymbol{x} = [\boldsymbol{q},\boldsymbol{\theta}]$, the control input vector is presented by $\boldsymbol{u} = [\boldsymbol{0},\boldsymbol{\tau}_m]$ in which $\boldsymbol{\tau}_m = [\tau_{m,1},..,\tau_{m,k}]$ is the vector of motor torques. The dynamic equations of the system is therefore expressed by

$$\mathbf{M}(\boldsymbol{q})\ddot{\boldsymbol{q}} + \boldsymbol{c}(\boldsymbol{q},\dot{\boldsymbol{q}}) + \boldsymbol{g}(\boldsymbol{q}) = \boldsymbol{\tau}_t(\phi,\dot{\phi}), \quad (3)$$

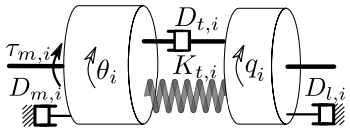


Figure 2: Mechanical model of $i-$th series viscoelastic actuator.

$$\mathbf{B}\ddot{\boldsymbol{\theta}} + \mathbf{D}_m\dot{\boldsymbol{\theta}} + \boldsymbol{\tau}_t(\phi,\dot{\phi}) = \boldsymbol{\tau}_m, \tag{4}$$

$$\boldsymbol{\tau}_t(\phi,\dot{\phi}) = \mathbf{K}_t\phi + \mathbf{D}_t\dot{\phi}, \tag{5}$$

where $\phi = \boldsymbol{\theta} - \boldsymbol{q}$ is the vector of transmission displacements; $\mathbf{B} = diag(B_1,...,B_k)$ is the inertia matrix of motors; $\mathbf{M}(\boldsymbol{q}) \in \Re^{k\times k}$ is the inertia matrix of links; $\boldsymbol{c}(\boldsymbol{q},\dot{\boldsymbol{q}}) \in \Re^k$ denotes the vector of Coriolis/centrifugal terms of links; $\boldsymbol{g}(\boldsymbol{q}) \in \Re^k$ denotes the gravitational torque of links; $\mathbf{D}_m = diag(D_{m,1},...,D_{m,k})$ presents the damping matrix associated with motors; $\boldsymbol{\tau}_t = [\tau_{t,1},..,\tau_{t,k}]$ is the vector of transmission torques applied by passive elements embedded in series with motors, with the constant stiffness of $\mathbf{K}_t = diag(K_{t,1},...,K_{t,k})$ and damping of $\mathbf{D}_t = diag(D_{t,1},...,D_{t,k})$.

# 3 CONTROL

The generic control task is the regulation of actuator torques of the manipulator $\boldsymbol{\tau}_m$ in such a way that the position of links $\boldsymbol{q}$ tracks a desired position $\boldsymbol{q}_d = [q_{d,1},..,q_{d,k}]$ while large positional errors are damped smoothly. First, the conventional position control of SEA-based manipulators is discussed.

## 3.1 Position Control

The position control of fully actuated manipulators can be done using a PID controller based on the error between the desired link position and the actual one, i.e. $\boldsymbol{e} = \boldsymbol{q}_d - \boldsymbol{q}$. It is principally feasible as it is a collocated feedback measured from the same DOF as the corresponding actuator. However, link positions are non-collocated feedbacks in flexible joint manipulators, and the control of these states in this way can cause instabilities (Cannon and Rosenthal, 1984). Hence, the stable link position control of flexible joint robots has been widely studied. A majority of these methods defines a set point according to the dynamic equations of links in static form

$$\frac{\partial \mathcal{U}(\boldsymbol{x})}{\partial \boldsymbol{q}} = \boldsymbol{g}(\boldsymbol{q}) - \mathbf{K}_t\phi = 0. \tag{6}$$

The most conventional method for the definition of control set point was introduced in (Tomei, 1991). This method is based on deriving the desired motor positions from the desired link positions using (6), i.e. $\boldsymbol{\theta}_d = \boldsymbol{q}_d + \mathbf{K}_t^{-1}\boldsymbol{g}(\boldsymbol{q}_d)$, and controlling these states using the corresponding collocated feedback $\boldsymbol{\theta}$, in addition to the compensation of the gravitational torque using a feedforward term. A more recent method suggested in (Albu-Schäffer et al., 2012) exploits the static link equations (6) to extract an equivalent value for the non-collocated states (link positions $\boldsymbol{q}$) using the collocated feedbacks (motor positions $\boldsymbol{\theta}$). For any given motor position $\boldsymbol{\theta}$, the equivalent link position $\bar{\boldsymbol{q}}$ is numerically obtained by solving (6), which was proved to have a unique solution due to the convex nature of potential energy function. Here, the Newton-Raphson method (Ben-Israel, 1966) is employed to solve (6). The equivalent link position $\bar{\boldsymbol{q}}$ is therefore iteratively computed from

$$\begin{aligned}\bar{\boldsymbol{q}}_j &= \bar{\boldsymbol{q}}_{j-1} - \left(\frac{\partial^2 \mathcal{U}(\bar{\boldsymbol{q}}_{j-1},\boldsymbol{\theta})}{\partial \boldsymbol{q}^2}\right)^{-1} \frac{\partial \mathcal{U}(\bar{\boldsymbol{q}}_{j-1},\boldsymbol{\theta})}{\partial \boldsymbol{q}} \\ &= \bar{\boldsymbol{q}}_{j-1} - \mathbf{J}_{\mathcal{U}}^{-1}(\bar{\boldsymbol{q}}_{j-1})\Big(\boldsymbol{g}(\bar{\boldsymbol{q}}_{j-1}) - \mathbf{K}_t\big(\boldsymbol{\theta} - \bar{\boldsymbol{q}}_{j-1}\big)\Big),\end{aligned} \tag{7}$$

where $j = 1,..,r$ is the iteration index, and $\mathbf{J}_{\mathcal{U}} \in \Re^{n\times n}$ denotes the passive stiffness of links which is obtained from

$$\mathbf{J}_{\mathcal{U}}(\boldsymbol{q}) = \mathbf{K}_t + \frac{\partial \boldsymbol{g}(\boldsymbol{q})}{\partial \boldsymbol{q}}. \tag{8}$$

Having the equivalent link position calculated after $r-$th iteration, i.e. $\bar{\boldsymbol{q}} = \bar{\boldsymbol{q}}_r$, its derivative can be also derived from

$$\dot{\bar{\boldsymbol{q}}} = \mathbf{J}_{\mathcal{U}}^{-1}(\bar{\boldsymbol{q}})\mathbf{K}_t\dot{\boldsymbol{\theta}}. \tag{9}$$

Using the equivalent of link position instead of the direct feedback, the potential instability issues caused by the non-collocated feedback is avoided as the equivalent value is obtained only from the collocated motor position feedback. Having employed this equivalent feedback, the proxy-based sliding mode position controller is presented below to derive the torque required to be applied on the manipulator links through the transmission systems.

## 3.2 Proxy-based Sliding Mode Control

As an extension to conventional Sliding mode and PID control methods, Proxy-based Sliding Mode Control method was introduced in (Kikuuwe et al., 2010) by exploiting the concepts of 'Proxy' and 'Virtual' Coupling from the haptic area. Fig. 3

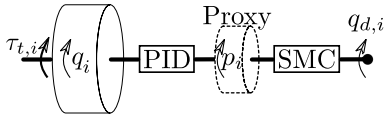

Figure 3: Physical interpretation of PSMC.

describes the physical idea behind this control approach. It is based on the connection of a virtual object, called proxy, to the output link by means of a virtual coupling that is implemented through a PID controller to maintain the link attached to the proxy; and the position of proxy is controlled using a Sliding Mode Controller (SMC) to track the desired link position. The fundamental benefit taken from this controller is the isolation of the 'local' and 'global' dynamics. While the local dynamics, i.e. the response to small position errors, is defined through the virtual coupling, the global dynamics, i.e the response to large position errors, is specified by the sliding mode controller. The PSMC approach can then provide an accurate tracking during normal operations with smooth recovery from large position errors resulting from undesigned interactions[1]. The proxy receives the torque from both the SMC controller and the virtual PID coupling, and the latter is defined as the reference torque $\boldsymbol{\tau}_r \in \Re^k$ to be exerted to the link through the motor.

By defining $\boldsymbol{p} = [p_1, .., p_k]$ as the vector of proxy positions, the torque $\boldsymbol{\tau}_{PID} \in \Re^k$ from the PID coupling is determined by

$$\boldsymbol{\tau}_{PID} = \mathbf{K}_P \dot{\boldsymbol{a}} + \mathbf{K}_I \boldsymbol{a} + \mathbf{K}_D \ddot{\boldsymbol{a}}, \tag{10}$$

where $\mathbf{K}_P$, $\mathbf{K}_I$ and $\mathbf{K}_D \in \Re^{k\times k}$ are diagonal positive definite matrices representing proportional, integral and derivative gains of virtual coupling, respectively, and $\boldsymbol{a}$ is the integral of the virtual coupling error. While this error was defined based on the link position for fully actuated manipulators, the equivalent link position $\bar{\boldsymbol{q}}$ is used here for flexible joint robots. It is then specified by

$$\boldsymbol{a} = \int (\boldsymbol{p} - \bar{\boldsymbol{q}}) dt. \tag{11}$$

The torque $\boldsymbol{\tau}_{SMC} \in \Re^k$ produced by the sliding mode controller, which is exploited for the control of proxy, is defined as follows

$$\boldsymbol{\tau}_{SMC} = \boldsymbol{\Gamma} sgn(\boldsymbol{s}), \tag{12}$$

where $\boldsymbol{\Gamma} \in \Re^{k\times k}$ is a diagonal matrix defining the torque limit of joints, $sgn(.)$ symbolizes the Signum function[2] acting on individual elements of the vector, and the sliding manifold $\boldsymbol{s} \in \Re^k$ is

$$\boldsymbol{s} = (\boldsymbol{q}_d - \boldsymbol{p}) + \boldsymbol{\Lambda}(\dot{\boldsymbol{q}}_d - \dot{\boldsymbol{p}}), \tag{13}$$

where $\boldsymbol{\Lambda} = diag(\lambda_1, .., \lambda_k)$ is a positive definite matrix specifying the time constant of the sliding surface of joints.

By introducing the auxiliary vector $\boldsymbol{\sigma}$ as

$$\boldsymbol{\sigma} = (\boldsymbol{q}_d - \bar{\boldsymbol{q}}) + \boldsymbol{\Lambda}(\dot{\boldsymbol{q}}_d - \dot{\bar{\boldsymbol{q}}}), \tag{14}$$

the SMC torque $\boldsymbol{\tau}_{SMC}$ from (12) can be rewritten as

$$\boldsymbol{\tau}_{SMC} = \boldsymbol{\Gamma} sgn(\boldsymbol{\sigma} - \dot{\boldsymbol{a}} - \boldsymbol{\Lambda}\ddot{\boldsymbol{a}}). \tag{15}$$

By setting the proxy mass to zero (Kikuuwe and Fujimoto, 2006), the dynamics of the proxy expresses the equality of torques from the SMC and the virtual PID coupling; and since the latter specifies the reference torque $\boldsymbol{\tau}_r$, it can be expressed using (10) and (15) as follows

$$\begin{aligned} \boldsymbol{\tau}_r &= \boldsymbol{\tau}_{PID} = \boldsymbol{\tau}_{SMC} \\ &= \mathbf{K}_P \dot{\boldsymbol{a}} + \mathbf{K}_I \boldsymbol{a} + \mathbf{K}_D \ddot{\boldsymbol{a}} \\ &= \boldsymbol{\Gamma} sgn(\boldsymbol{\psi} - \boldsymbol{\Lambda}\ddot{\boldsymbol{a}}), \end{aligned} \tag{16}$$

where $\boldsymbol{\psi} = \boldsymbol{\sigma} - \dot{\boldsymbol{a}}$ is an auxiliary vector. With considering the mathematical relation[3]

$$\begin{aligned} \delta &= \beta + \gamma sgn(\rho - \kappa\delta) \\ &= \beta + \gamma sat\left(\frac{\rho}{\kappa\gamma} - \frac{\beta}{\gamma}\right), \end{aligned} \tag{17}$$

where $\delta$, $\beta$, $\gamma$, $\rho$ and $\kappa$ are arbitrary variables, and $sat(.)$ symbolizes the Saturation function[4], (16) can be solved for $\ddot{\boldsymbol{a}}$ as follows

$$\begin{aligned} \ddot{\boldsymbol{a}} = &-\mathbf{K}_D^{-1}(\mathbf{K}_P \dot{\boldsymbol{a}} + \mathbf{K}_I \boldsymbol{a}) + \\ &\mathbf{K}_D^{-1} \boldsymbol{\Gamma} sat\left(\boldsymbol{\Gamma}^{-1}\left(\mathbf{K}_D \boldsymbol{\Lambda}^{-1} \boldsymbol{\psi} + \mathbf{K}_P \dot{\boldsymbol{a}} + \mathbf{K}_I \boldsymbol{a}\right)\right), \end{aligned} \tag{18}$$

in which the saturation function acts on individual elements of the given vector. By adding the gravity compensation feed-forward torque, the reference torque can therefore be obtained from

$$\boldsymbol{\tau}_r = \boldsymbol{\Gamma} sat\left(\boldsymbol{\Gamma}^{-1}\left(\mathbf{K}_D \boldsymbol{\Lambda}^{-1} \boldsymbol{\psi} + \mathbf{K}_P \dot{\boldsymbol{a}} + \mathbf{K}_I \boldsymbol{a}\right)\right) + \boldsymbol{g}(\bar{\boldsymbol{q}}). \tag{19}$$

In order to execute the proxy-based sliding mode position controller, the above torque needs to be exerted to links. Hence, a torque controller is employed, which is expressed as follows.

[1]This problem can be also solved using motion planning provided that the system can sense 'unforeseen' events, however the sensory information is not usually available.

[2]The Signum of an arbitrary variable $\xi$ is defined as $sgn(\xi) = \frac{\xi}{|\xi|}$ which is undefined at $\xi = 0$.

[3]This relation can be simply proved from $\delta = sgn(\rho - \delta) \Leftrightarrow \delta = sat(\rho)$.

[4]The Saturation or Clipping function of an arbitrary variable $\xi$ is defined as $sat(\xi) = \frac{\xi}{max(1,|\xi|)}$.

### 3.3 Torque Control

A torque controller is designed in this section in order to track the reference torque given by the Proxy-based Sliding Mode Controller. (Vertechy et al., 2010) studied a torque control approach for single flexible joints based on the Linear-Quadratic optimal method, and presented the tracking performance achieved by the proposed scheme in comparison with other approaches. A similar approach extended for flexible joint manipulators is presented in this work.

By subtracting the angular acceleration of motors $\ddot{\boldsymbol{q}}$ from that of links $\ddot{\boldsymbol{\theta}}$, using (3)-(5), it can be shown that

$$\ddot{\phi}+\mathbf{B}^{-1}\mathbf{D}_m\dot{\boldsymbol{\theta}}-\mathbf{M}^{-1}(\boldsymbol{q})\boldsymbol{g}(\boldsymbol{q}) + \left(\mathbf{B}^{-1}+\mathbf{M}^{-1}(\boldsymbol{q})\right)(\mathbf{K}_t\phi+\mathbf{D}_t\dot{\phi})=\mathbf{B}^{-1}\boldsymbol{\tau}_0, \tag{20}$$

where $\boldsymbol{\tau}_0\in\Re^k$ is the motor torque associated with the system dynamics when the Coriolis/centrifugal terms are not considered. It is neglected on the basis that the system is meant for human-robot interaction and the fast motion of links is strictly avoided due to safety requirements (Haddadin et al., 2009). Defining the Feedback Linearization controller as

$$\boldsymbol{\tau}_0=\mathbf{B}\mathbf{M}^{-1}(\boldsymbol{q})\left(\mathbf{K}_t\phi+\mathbf{D}_t\dot{\phi}-\boldsymbol{g}(\boldsymbol{q})\right)+\mathbf{D}_m\dot{\boldsymbol{\theta}}+\mathbf{B}\boldsymbol{v}, \tag{21}$$

the dynamic equation of the transmission (20) is rewritten as

$$\ddot{\phi}+\check{\mathbf{K}}_t\phi+\check{\mathbf{D}}_t\dot{\phi}=\boldsymbol{v}, \tag{22}$$

where $\boldsymbol{v}\in\Re^k$ is the new control input for the linear dynamic system (22), $\check{\mathbf{K}}_t=\mathbf{B}^{-1}\mathbf{K}_t$ and $\check{\mathbf{D}}_t=\mathbf{B}^{-1}\mathbf{D}_t$.

The control problem is then to design $\boldsymbol{v}\in\Re^k$ in a way that the transmission torque $\boldsymbol{\tau}_t$ tracks the reference value $\boldsymbol{\tau}_r$ given by the PSMC. By defining a new state vector $\boldsymbol{w}=[\phi,\dot{\phi}]\in\Re^{2k}$, the linear system (22) can be expressed in state-space form as follows

$$\begin{cases}\dot{\boldsymbol{w}}=\mathbf{A}\boldsymbol{w}+\mathbf{F}\boldsymbol{v}\\ \boldsymbol{\tau}_t=\mathbf{C}\boldsymbol{w}\end{cases}, \tag{23}$$

where $\mathbf{A}=[[\mathbf{0}_{k\times k},-\check{\mathbf{K}}_t]^T,[\mathbf{I}_k,-\check{\mathbf{D}}_t]^T]\in\Re^{2k\times 2k}$ is the state matrix in which $\mathbf{0}_{k\times k}$ and $\mathbf{I}_k$ symbolize the zero and the identity matrices with the dimension of $k\times k$, $\mathbf{F}=[\mathbf{0}_{k\times k},\mathbf{I}_k]^T\in\Re^{2k\times k}$ is the input matrix, and $\mathbf{C}=[\mathbf{K}_t,\mathbf{D}_t]\in\Re^{k\times 2k}$ is the output matrix. The control law is chosen as (Aström and Murray, 2010)

$$\boldsymbol{v}=\boldsymbol{v}_{ff}+\boldsymbol{v}_{fb}, \tag{24}$$

where $\boldsymbol{v}_{ff}\in\Re^k$ and $\boldsymbol{v}_{fb}\in\Re^k$ are the feedforward and feedback part of the controller. The feedforward term does not change the stability of the system, although it can affect the steady-space solution. This term is then derived by setting the desired output value to the steady state output for the close-loop system. Given a constant torque reference, this is defined by

$$\boldsymbol{v}_{ff}=\mathbf{B}^{-1}\boldsymbol{\tau}_r. \tag{25}$$

The feedback term is designed using a LQ optimal controller based on the described system augmented with the integral of the tracking error which is defined by

$$\tilde{\boldsymbol{\tau}}_I=\int(\boldsymbol{\tau}_r-\boldsymbol{\tau}_t)dt. \tag{26}$$

The augmented system can then be described by

$$\begin{cases}\dot{\bar{\boldsymbol{w}}}=\bar{\mathbf{A}}\bar{\boldsymbol{w}}+\bar{\mathbf{F}}\boldsymbol{v}-\mathbf{H}\boldsymbol{\tau}_r\\ \boldsymbol{\tau}_t=\mathbf{C}\bar{\boldsymbol{w}}\end{cases}, \tag{27}$$

where $\bar{\mathbf{A}}=[[\mathbf{A}^T,-\mathbf{C}^T]^T,[\mathbf{0}_{k\times 3k}]^T]\in\Re^{3k\times 3k}$, $\bar{\boldsymbol{w}}=[\boldsymbol{w},\tilde{\boldsymbol{\tau}}_I]\in\Re^{3k}$, $\bar{\mathbf{F}}=[\mathbf{F}^T,\mathbf{0}_{k\times k}]^T\in\Re^{3k\times k}$ and $\mathbf{H}=[\mathbf{0}_{k\times 2k},\mathbf{I}_k]^T\in\Re^{3k\times k}$. The feedback control law is then defined by

$$\boldsymbol{v}_{fb}=-\mathbf{K}_{LQ}\bar{\boldsymbol{w}}. \tag{28}$$

where $\mathbf{K}_{LQ}\in\Re^{3k\times 3k}$ is the gain matrix designed using the LQ optimal method. It is based on finding the control feedback $\boldsymbol{v}_{fb}$ that minimizes the performance index $J_{LQ}$ which is expressed by

$$J_{LQ}=\int_0^\infty e^{2\mu t}\left(\bar{\boldsymbol{w}}^T(t)\mathbf{Q}\bar{\boldsymbol{w}}(t)+\boldsymbol{v}_{fb}^T(t)\mathbf{R}\boldsymbol{v}_{fb}(t)\right)dt \tag{29}$$

where $\mathbf{Q}\in\Re^{3k\times 3k}$ and $\mathbf{R}\in\Re^{k\times k}$ are positive definite matrices defining the weights of states and the feedback control inputs, respectively; and $\mu>0$ is a constant specifying the degree of stability. By finding the matrix $\mathbf{P}\in\Re^{3k\times 3k}$ from the algebraic Riccati equation

$$\bar{\mathbf{A}}^T\mathbf{P}+\mathbf{P}\bar{\mathbf{A}}+2\mu\mathbf{P}+\mathbf{Q}=\mathbf{P}\bar{\mathbf{F}}\mathbf{R}^{-1}\bar{\mathbf{F}}^T\mathbf{P}, \tag{30}$$

the gain matrix is obtained as $\mathbf{K}_{LQ}=\mathbf{R}^{-1}\bar{\mathbf{F}}^T\mathbf{P}$. Due to decoupling characteristic of the linear dynamic system (22), it can be shown that the gain $\mathbf{K}_{LQ}$ is a diagonal matrix and it can be expressed as $\mathbf{K}_{LQ}=diag(\mathbf{K}_\phi,\mathbf{K}_{\dot{\phi}},\mathbf{K}_{\tilde{\tau}_I})$ in which $\mathbf{K}_\phi$, $\mathbf{K}_{\dot{\phi}}$ and $\mathbf{K}_{\tilde{\tau}_I}\in\Re^{k\times k}$ are auxiliary diagonal matrices corresponding to $\phi$, $\dot{\phi}$ and $\tilde{\boldsymbol{\tau}}_I$, respectively.

By adding the active damping $\mathbf{D}_a\in\Re^{k\times k}$ on the motion of motor, and using the equivalent link position instead of the actual one in order to avoid using the non-collocated feedback, the overall torque control law can accordingly be expressed by

$$\boldsymbol{\tau}_m=\boldsymbol{\tau}_r+(\mathbf{D}_m-\mathbf{D}_a)\dot{\boldsymbol{\theta}}-\mathbf{B}\mathbf{K}_{\tilde{\tau}_I}\tilde{\boldsymbol{\tau}}_I+ \mathbf{B}\mathbf{M}^{-1}(\bar{\boldsymbol{q}})\left(\mathbf{K}_t\phi+\mathbf{D}_t\dot{\phi}-\boldsymbol{g}(\bar{\boldsymbol{q}})\right)-\mathbf{B}\mathbf{K}_\phi\phi-\mathbf{B}\mathbf{K}_{\dot{\phi}}\dot{\phi}, \tag{31}$$

in which $\boldsymbol{\tau}_r$ is the reference torque given by the PSMC approach (19).

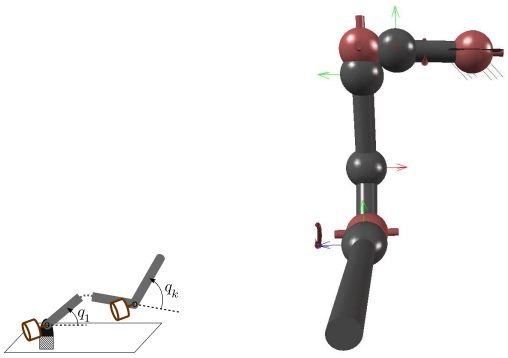


(a) (b)

Figure 4: The arm employed for simulations (a) the real hardware (b) MapleSim model.

# 4 SIMULATIONS

## 4.1 System Description

The manipulator simulated to evaluate the performance of presented approach is an anthropomorphic arm introduced in (Laffranchi et al., 2013; Kashiri et al., 2013a), powered by compliant actuators benefiting from variable physical damping in parallel with series elasticity (Laffranchi et al., 2011), see Fig. 2. The physical damping of this system is generated using a clutch mechanism driven by a set of four piezo-electric actuators. Having controlled the clutch force (Lee et al., 2014), a target viscous damping behavior can be replicated (Kashiri et al., 2014a), or a mechanical fuse can be executed to provide both accuracy and safety (Kashiri et al., 2014b). An image of the real manipulator beside that of the MapleSim model employed for simulations is illustrated in Fig. 4. The stiffness of joints are specified using the approach proposed in (Kashiri et al., 2013b); setting that of first two joints to 188 N.m/rad, and that of last two joints to 103 N.m/rad.

## 4.2 Simulation Results

In this section, the performance of the presented control scheme is demonstrated in two simulations in comparison with the PD controller proposed in (Albu-Schäffer et al., 2012). The PID control gains of PSMC are chosen as $\mathbf{K}_P = diag(200,200,100,100)$ and $\mathbf{K}_D = diag(50,50,20,20)$ while the position integrator is not considered, i.e. $\mathbf{K}_I = diag(0,0,0,0)$, to present a plausible comparison with the aforesaid existing method. The torque controller gains $\mathbf{K}_{LQ}$ are obtained based on the choice of $\mathbf{Q} = diag(10^3\mathbf{K}_t, 10^2\mathbf{D}_t, 10\mathbf{I}_4)$, $\mathbf{R} = \mathbf{I}_4$ and $\mu = 1$. The active damping of the torque controller is also selected as $\mathbf{D}_a = diag(20,20,10,10)$. The homing position of the arm at rest (zero velocity) is considered as the initial state of the system.

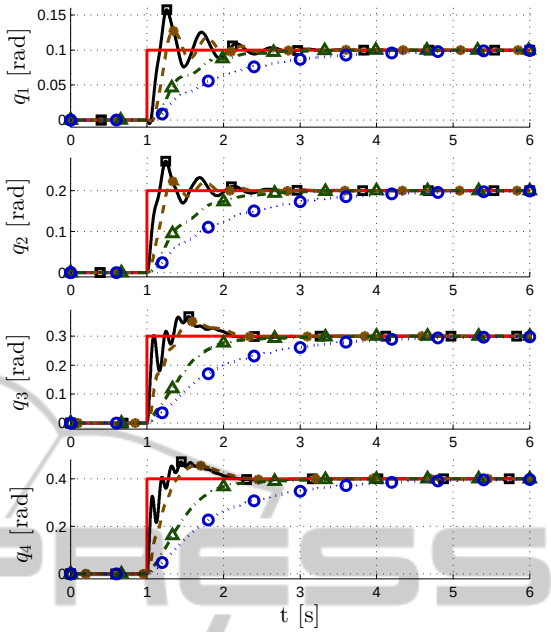


Figure 5: Step response of the system with different values of the time constant: $\lambda = 0.1$ in (—∗), $\lambda = 0.5$ in (-.-△), $\lambda = 1.0$ is in (---◯). The reference position is in red line (—), and the response of the system using the PD controller is in (—□).

### 4.2.1 Step Response

The first simulation presents the step response of the manipulator when it is controlled using the PSMC, and it is compared with the PD controller. This test was carried out considering different time constant values of $\Lambda = \lambda\mathbf{I}_4$ with $\lambda = 0.1$, $\lambda = 0.5$ and $\lambda = 1$ to present the effect of the sliding mode parameter on the response of the system. Fig. 5 demonstrates changes in link positions versus time. The improvement achieved by the PSMC scheme in compared to PD controller can be clearly seen as the system tracks the desired position with a smooth and over-damped behavior. It can be seen that the growth of the factor $\lambda$ amplifies the damping behavior of the system, although it also reduces the settling time of the system. Hence, the maximum value of this factor should be specified according to the minimum bandwidth required for the response of the system.

### 4.2.2 Sinusoidal Trajectory Tracking

This simulation is carried out to show the tracking performance achieved by the controller. The

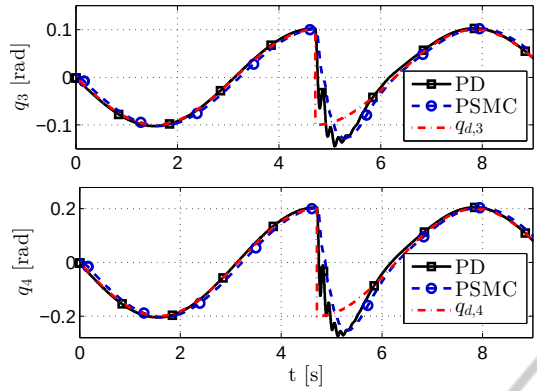


Figure 6: Time history of link positions; desired values in compared to actual ones when the system is controlled by PSMC and PD.

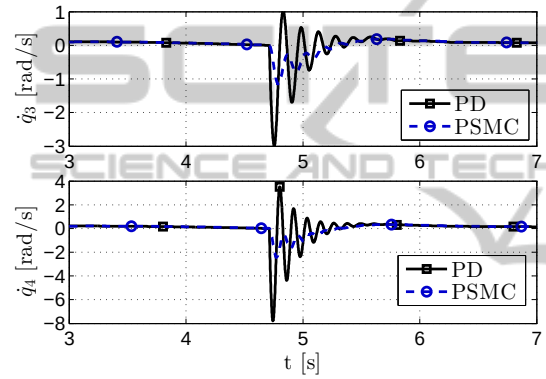


Figure 7: Time history of link velocities when the system is controlled by PSMC in compared to that by PD.

task considered for this simulation is to track a sinusoidal reference in elbow joints ($i = 3,4$) while a discontinuity in desired position is imposed in order to evaluate the response of the system to large positional errors. For the sake of clarity, only a time constant of $\lambda = 0.1$ is considered for this simulation. Fig. 6 illustrates changes in link positions versus time when the systems is controlled by PSMC in compared to that by PD. It can be seen that the PSMC approach represents a tracking performance quite similar to the conventional PD controller when the reference trajectory is continuous and smooth, and the use of PSMC hardly affect the control performance; however, in the case of unforeseen events leading to a large positional discontinuity, the conventional PD controller shows considerable oscillations while the PSMC recovers smoothly, although the increase of the time constant $\lambda$ can amplify the damping behavior achieved by the PSMC (as shown in previous simulation). The difference in performance of these controllers can be seen more clearly in link velocities and motor torques which are illustrated in Fig. 7 and Fig. 8, respectively. When the reference position

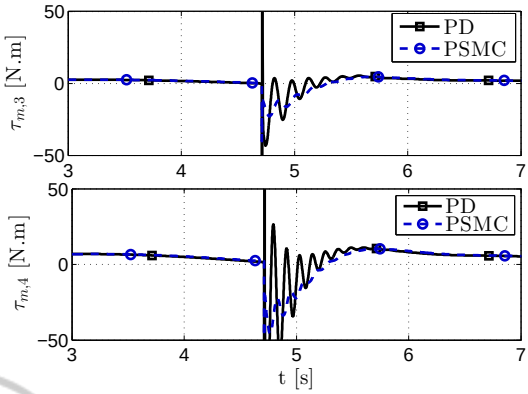


Figure 8: Time history of motor torques when the system is controlled by PSMC in compared to that by PD.

changes smoothly, change in the motor torques and the link velocities resulting from both controllers are also quite smooth and reasonable. However, large positional errors (shown in Fig. 6 at $t = 2.7$s) in a torque-limited PD controller result in very high motor torques with substantial changes leading to significant oscillations in link velocities; while the employment of the PSMC moves the proxy in such a way that the target position of the PSMC's PD controller moves gently. This provides a plausible change in motor torques and a smooth damping of the link motion. It should be noted that the increase of the derivative action, i.e. D-gains of the PID controller, would theoretically replicate the same behavior; however it is not practically feasible due to typical noise in velocity feedbacks.

## 5 CONCLUSIONS

In the trend towards friendly human-robot interaction, Proxy-based Sliding Model Control approach was introduced to maintain proper tracking performance in normal operations while showing a smooth and safe response to undesigned interactions. However, the study of this approach for flexible joint robots had not been discussed. This paper proposed a control scheme to exploit this method for this class of underactuated systems. The PSMC approach formulation was adopted according to stability requirements of flexible joint manipulators; and in order to implement this controller on flexible joint robots, a novel torque controller based on the Feedback Linearization approach and the Linear Quadratic Optimal control method was presented. Finally, the performance of the proposed scheme was demonstrated in dynamic simulations of a flexible joint manipulator to represent the improvement

achieved by this controller in compared to a conventional PID approach. The future work of the authors will include the implementation of the proposed approach on the real arm to validate the performance of this scheme in experimental results.

## ACKNOWLEDGEMENTS

This work is supported by the European Research Council under EU FP7-ICT projects SAPHARI no. 287513 and WALKMAN no. 611832.

## REFERENCES

Albu-Schäffer, A., Petit, F., and Ott, C. (2012). Energy Shaping Control for a Class of Underactuated Euler-Lagrange Systems. In Petrovic, I. and Korondi, P., editors, *10th IFAC Symposium on Robot Control*, Dubrovnik, Croatia.

Aström, K. J. and Murray, R. M. (2010). *Feedback systems: an introduction for scientists and engineers*. Princeton university press.

Ben-Israel, A. (1966). A Newton-Raphson method for the solution of systems of equations. *Journal of Mathematical analysis and applications*, 15(2):243–252.

Beyl, P., Van Damme, M., Van Ham, R., Vanderborght, B., and Lefeber, D. (2009). Design and control of a lower limb exoskeleton for robot-assisted gait training. *Applied Bionics and Biomechanics*, 6(2):229–243.

Bicchi, A., Rizzini, S. L., and Tonietti, G. (2001). Compliant design for intrinsic safety: General issues and preliminary design. In *Intelligent Robots and Systems, 2001. Proceedings. 2001 IEEE/RSJ International Conference on*, volume 4, pages 1864–1869. IEEE.

Braun, D. J., Petit, F., Huber, F., Haddadin, S., Van Der Smagt, P., Albu-Schaffer, A., and Vijayakumar, S. (2013). Robots driven by compliant actuators: Optimal control under actuation constraints. *IEEE Transactions on Robotics*, 29(5):1085–1101.

Cannon, R. H. and Rosenthal, D. E. (1984). Experiments in control of flexible structures with noncolocated sensors and actuators. *Journal of Guidance, Control, and Dynamics*, 7(5):546–553.

Catalano, M. G., Grioli, G., Garabini, M., Bonomo, F., Mancini, M., Tsagarakis, N., and Bicchi, A. (2011). VSA-CubeBot: A modular variable stiffness platform for multiple degrees of freedom robots. In *Proceedings - IEEE International Conference on Robotics and Automation*, pages 5090–5095.

Chen, L., Garabini, M., Laffranchi, M., Kashiri, N., Tsagarakis, N. G., Bicchi, A., and Caldwell, D. G. (2013a). Optimal Control for Maximizing Velocity of the CompAct Compliant Actuator. In *Robotics and Automation (ICRA), 2013 IEEE International Conference on*, pages 516–522, Karlsruhe (Germany).

Chen, L., Laffranchi, M., Lee, J., Kashiri, N., Tsagarakis, N. G., and Caldwell, D. G. (2013b). Link position control of a compliant actuator with unknown transmission friction torque. In *Intelligent Robots and Systems (IROS), 2013 IEEE/RSJ International Conference on*, pages 4058–4064. IEEE.

De Luca, A., Siciliano, B., and Zollo, L. (2005). PD control with on-line gravity compensation for robots with elastic joints: Theory and experiments. *Automatica*, 41(10):1809–1819.

Garcia, E., Arévalo, J. C., Muñoz, G., and Gonzalez-de Santos, P. (2011). Combining series elastic actuation and magneto-rheological damping for the control of agile locomotion. *Robotics and Autonomous Systems*, 59(10):827–839.

Haddadin, S., Albu-Schäffer, A., and Hirzinger, G. (2009). Requirements for safe robots: Measurements, analysis and new insights. *The International Journal of Robotics Research*, 28(11-12):1507–1527.

Kashiri, N., Laffranchi, M., Lee, J., Tsagarakis, N. G., Chen, L., and Caldwell, D. (2014a). Real-time damping estimation for variable impedance actuator. In *Robotics and Automation (ICRA), 2014 IEEE International Conference on*, pages 1072–1077. IEEE.

Kashiri, N., Laffranchi, M., Tsagarakis, N. G., Margan, A., and Caldwell, D. G. (2014b). Physical Interaction Detection and Control of Compliant Manipulators Equipped with Friction Clutches. In *Robotics and Automation (ICRA), 2014 IEEE International Conference on*, pages 1066–1071. IEEE.

Kashiri, N., Laffranchi, M., Tsagarakis, N. G., Sardellitti, I., and Caldwell, D. G. (2013a). Dynamic modeling and adaptable control of the CompAct arm. In *Mechatronics (ICM), 2013 IEEE International Conference on*, pages 477–482.

Kashiri, N., Tsagarakis, N. G., Laffranchi, M., and Caldwell, D. G. (2013b). On the stiffness design of intrinsic compliant manipulators. In *Advanced Intelligent Mechatronics (AIM), 2013 IEEE/ASME International Conference on*, pages 1306–1311. IEEE.

Kikuuwe, R. and Fujimoto, H. (2006). Proxy-based sliding mode control for accurate and safe position control. In *Robotics and Automation, 2006. ICRA 2006. Proceedings 2006 IEEE International Conference on*, pages 25–30. IEEE.

Kikuuwe, R., Yasukouchi, S., Fujimoto, H., and Yamamoto, M. (2010). Proxy-based sliding mode control: a safer extension of PID position control. *Robotics, IEEE Transactions on*, 26(4):670–683.

Laffranchi, M., Tsagarakis, N., and Caldwell, D. G. (2011). A compact compliant actuator (CompAct) with variable physical damping. In *Robotics and Automation (ICRA), 2011 IEEE International Conference on*, pages 4644–4650. IEEE.

Laffranchi, M., Tsagarakis, N. G., and Caldwell, D. G. (2013). CompAct Arm: a Compliant Manipulator

with Intrinsic Variable Physical Damping. *Robotics: Science and Systems VIII*, page 225.

Lee, J., Laffranchi, M., Kashiri, N., Tsagarakis, N., and Caldwell, D. (2014). Model-Free Force Tracking Control of Piezoelectric Actuators: Application to Variable Damping Actuator. In *Robotics and Automation, 2014. ICRA'14. IEEE International Conference on*, pages 2283–2289.

Mathijssen, G., Brackx, B., Van Damme, M., Lefeber, D., and Vanderborght, B. (2013). Series-Parallel Elastic Actuation (SPEA) with intermittent mechanism for reduced motor torque and increased efficiency. In *Intelligent Robots and Systems (IROS), 2013 IEEE/RSJ International Conference on*, pages 5841–5846. IEEE.

Ortega, R. (1998). *Passivity-based Control of Euler-Lagrange Systems: Mechanical, Electrical and Electromechanical Applications*. Communications and Control Engineering. Springer.

Ozgoli, S. and Taghirad, H. D. (2006). A survey on the control of flexible joint robots. *Asian Journal of Control*, 8(4):332–344.

Paluska, D. and Herr, H. (2006). The effect of series elasticity on actuator power and work output: Implications for robotic and prosthetic joint design. *Robotics and Autonomous Systems*, 54(8):667–673.

Prieto, P. J., Rubio, E., Hernández, L., and Urquijo, O. (2013). Proxy-based sliding mode control on platform of 3 degree of freedom (3-DOF). *Advanced Robotics*, 27(10):773–784.

Radulescu, A., Howard, M., Braun, D. J., and Vijayakumar, S. (2012). Exploiting variable physical damping in rapid movement tasks. In *Advanced Intelligent Mechatronics (AIM), 2012 IEEE/ASME International Conference on*, pages 141–148. IEEE.

Tomei, P. (1991). A simple PD controller for robots with elastic joints. *Automatic Control, IEEE Transactions on*, 36(10):1208–1213.

Tsagarakis, N. G., Laffranchi, M., Vanderborght, B., and Caldwell, D. G. (2009). A compact soft actuator unit for small scale human friendly robots. In *Robotics and Automation, 2009. ICRA'09. IEEE International Conference on*, pages 4356–4362. IEEE.

Tsagarakis, N. G., Sardellitti, I., and Caldwell, D. G. (2011). A new variable stiffness actuator (CompAct-VSA): Design and modelling. In *Intelligent Robots and Systems (IROS), 2011 IEEE/RSJ International Conference on*, pages 378–383. IEEE.

Van Damme, M., Vanderborght, B., Verrelst, B., Van Ham, R., Daerden, F., and Lefeber, D. (2009). Proxy-based sliding mode control of a planar pneumatic manipulator. *The International Journal of Robotics Research*, 28(2):266–284.

Vanderborght, B., Albu-Schaeffer, A., Bicchi, A., Burdet, E., Caldwell, D. G., Carloni, R., Catalano, M., Eiberger, O., Friedl, W., Ganesh, G., Garabini, M., Grebenstein, M., Grioli, G., Haddadin, S., Hoppner, H., Jafari, A., Laffranchi, M., Lefeber, D., Petit, F., Stramigioli, S., Tsagarakis, N., Van Damme, M., Van Ham, R., Visser, L. C., and Wolf, S. (2013). Variable impedance actuators: A review. *Robotics and Autonomous Systems*, 61:1601–1614.

Vanderborght, B., Tsagarakis, N. G., Van Ham, R., Thorson, I., and Caldwell, D. G. (2011). MACCEPA 2.0: Compliant actuator used for energy efficient hopping robot Chobino1D. *Autonomous Robots*, 31:55–65.

Vertechy, R., Frisoli, A., Solazzi, M., Dettori, A., and Bergamasco, M. (2010). Linear-quadratic-Gaussian torque control: Application to a flexible joint of a rehabilitation exoskeleton. In *Robotics and Automation (ICRA), 2010 IEEE International Conference on*, pages 223–228. IEEE.